FURTHER SEARCHES FOR LUNAR ICE IN CLEMENTINE BISTATIC RADAR DATA.

R.A. Simpson, Packard Building - Room 332, Stanford University, Stanford, CA 94305-9515 (rsimpson@magellan.stanford.edu)

Introduction: Nozette *et al.* [1] analyzed Clementine bistatic radar data and concluded that enhancements in scattered signal from the lunar surface could be detected when (1) the bistatic angle β approached 0° and (2) the surface region primarily responsible for the echo had the highest fraction of permanently shaded terrain. On the basis of this detection, they inferred possible presence of water ice deposits near the South Pole. We subsequently examined the same data and were unable to reproduce their results [2]. Nozette and colleagues have since criticized our analysis on several grounds (*e.g.*, [3]). We address some of the criticisms here, but have found no reason to change our conclusions.

Issues: The criticisms fall into two broad categories. Nozette and colleagues have argued that we did not correctly estimate the quantity of ice that could be present based on their detection (or an upper limit, based on our lack of a detection). Estimating the quantity of ice is very difficult given that its scattering is expected to be strongly dependent on purity and burial depth. There is little more we can contribute at this time, so we focus here on the second set of criticisms.

These other criticisms concern the completeness of our analysis. We did not compute the ratio of scattered power in the two orthogonal received polarizations as a function $r(\beta)$ and did not optimize its response in terms of the percentage of shaded terrain within the radar "footprint." Nozette *et al.* [3] have argued that the echo power ratio $r(\beta)$ must be derived "as a phase function for the entire south pole region. It was this function that showed enhancement, not just a few individual Doppler bins." On the other hand, Nozette *et al.* [4] have contended that "approximately 2.4-18.3 km^2 of relatively clean ice is present near the surface and on the wall of Shackleton crater and in at least one of the neighboring dark areas." We saw nothing in our original analysis to justify calculation of a phase function $r(\beta)$ either broadly for the polar region or for any subset of its area. With the recent prompting from Nozette and colleagues, however, we have carried out several such derivations.

Analysis: The bistatic radar data are most conveniently analyzed as time-ordered pairs of power spectra—one for right-circular polarization (RCP) and the other for left (LCP). In our case we used 16384 complex (I/Q) time samples from each receiver channel to compute individual spectra with time and frequency resolutions of approximately 0.6 s and 1.5 Hz, respectively. One can take the RCP/LCP ratio immediately or compute average spectra within each channel before finding the ratio; we have done both.

For each 0.6 s time step and each 1.5 Hz frequency bin one can identify a corresponding strip (Doppler contour) on the lunar surface. The mapping of frequencies to strips is dynamic; the size and shape of strips is continually changing as the spacecraft moves in its orbit. But the variations are well-behaved and interpolations among fiducial points are straightforward. It is then possible to associate each power measurement in a spectrum with one of these Doppler strips (not a point) on the surface.

Each Doppler contour highlights the surface area contributing echo power to a single frequency bin in a power spectrum. Over a Doppler strip the range of corresponding bistatic angles β can be several degrees, but there will be a minimum β_{min} for each contour. For observations near the South Pole, β_{min} occurs very near the locus of points where $\beta=0$. We selected a set of 72 $\beta=0°$ points on the surface, spaced by 1 s in time and poleward of 80°S (see Figure 2 in [2]), which we defined to be "reference targets" for generation of empirical scattering functions. We then assigned measured powers in each spectrum to these empirical functions $\sigma_R(\beta)$, $\sigma_L(\beta)$, and $r(\beta)$ corresponding to right-, left-, and ratio values at each target. The frequency and time of the value determined the reference target assignment; the instantaneous geometry determined the β angle at that target. The range of β for these functions was chosen to be ±5° in steps of 0.1°.

Many of the data points were mapped to surface areas outside the polar region; others were beyond our limit $|\beta|<5°$. Nevertheless, we assigned over 50000 points to each of the 3x72 empirical scattering functions. Most bins had 10 or more points; the maximum was 42. A few bins, owing to unfavorable geometry or our limitation of processing to 16 minutes of data approximately centered on South Pole backscatter [2], had no values. As an aside, we note that these are weak signals; the scatter in data values (particularly the ratios) is considerable.

From analysis of image data, Nozette *et al.* [1] found that Doppler contours having maximum overlap with permanently shadowed terrain yielded the strongest enhancement near $\beta=0$. From Fig. 4 in [1] and Fig. 1 in [4] we have inferred that this surface area corresponds to our reference targets numbered 58 to 70 – targets poleward of approximately 88°S. We combined the empirically derived scattering functions for these targets and obtained the results shown in Fig. 1. Curve (a) shows the average RCP for each β value divided by the average LCP; Curve (b) shows the median of individual RCP/LCP values at each β.

There are a number of other ways to combine median and averaging operations, and we investigated

several including functions equivalent to those shown in Fig. 1 but using all 72 reference targets and to another set in which we used the most southerly 22 targets. We also examined two-dimensional displays of scattered power versus β in one dimension and target number in the other. As in Fig. 1, there was no case where either the scattered power or the ratio of scattered powers peaked around β=0.

Conclusion: We reported no evidence for enhanced backscatter in our original analysis [2]. After following the suggestions of Nozette and colleagues that we construct scattering functions as a function of β, we continue to see no such evidence. This result applies to individual receiver channels, their ratio, for many frequency bins near the pole, for what we believe to be the same frequency bins as selected by Nozette and colleagues, for individual frequency bins, for calculations using averages, and for calculations using median functions. As noted previously [2], these results do not prove the absence of water ice on the Moon. But they do suggest that it was not detected during the Clementine bistatic radar experiment.

References: [1] Nozette S. and 8 co-authors (1996) *Science*, *274*, 1495-1498. [2] Simpson R.A. and G.L. Tyler (1999) *JGR*, *104*, 3845-3862. [3] Nozette S. and 4 co-authors (1998) *LPI Contribution No. 958*, 60-61. [4] Nozette S. and 5 co-authors (1999) *LPSC XXX*, 1665-1666.

recession. The scattering function resolution is 0.1° in β with about 40 measurements per bin near β=-4° and about 250 points per bin near β=+4°. The range 4°<|β|<5° was poorly sampled. (a) Solid line shows ratio of the average RCP value to the average LCP value at each angle. (b) Dotted line shows median of individual RCP/LCP ratios.
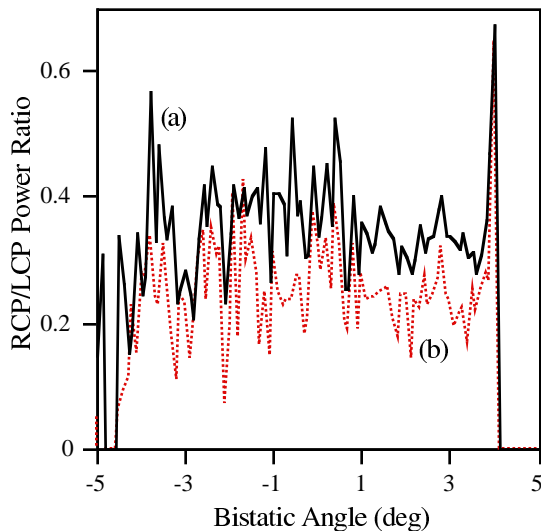

Fig. 1: Two scattering functions derived from Clementine bistatic radar power spectra near the lunar South Pole. Neither shows the enhancement near β=0 that would be expected from significant exposures of clean water ice. In both cases the function is based on the composite response of 13 reference target points poleward of about 88°S. Negative values of β denote approach to the β=0 condition for the target; positive values denote